1.19

GLOBAL FORECASTS OF THERMOSPHERIC GRAVITY WAVE ACTIVITY AS GENERATED FROM TROPOSPHERIC SOURCES: AN OVERVIEW OF THE FOREGRATS MODEL WITH APPLICATION TO THE PREDICTION OF EQUATORIAL SPREAD-F

Timothy J. Kane[1*], Andrew J. Gerrard[2], Alexander Hassiotis[1]

[1] The Pennsylvania State University, University Park, Pennsylvania
[2] Clemson University, Clemson, South Carolina

1. ABSTRACT

Atmospheric gravity waves, generated primarily from tropospheric mesoscale convective complexes and frontal systems, propagate into the middle atmosphere and subsequently impact the entire global circulation. Furthermore, the short-period/long vertical wavelength portion of the gravity wave spectrum can propagate into the thermosphere, where such waves can potentially "seed" equatorial spread-F (ESF), an instability phenomena which causes scintillation in the radio portion of the electromagnetic spectrum. Recently, the desire to acquire 4-6 hour forecasts of ESF has come to the forefront of upper atmospheric research because of the impacts on radio communications and GPS signals. However, to extend these forecasts beyond the 6 hour limit, the modeling of the synoptic gravity waves associated with ESF needs to be addressed. As such, in this paper we present a global gravity wave forecasting model called FOREGRATS (FOREcasting of Gravity waves via Ray-tracing algorithms with prescribed Tropospheric Sources), which uses a myriad of data resources to identify dominant tropospheric gravity wave sources, prescribe a relevant source spectrum, and then propagate the resultant gravity waves through the middle and upper atmosphere via a linear ray-tracing theory. An example of the entire data assimilation and forecasting processes is presented, outlining each of the major components of the model.

2. INTRODUCTION

The low-latitude (i.e., geographic latitude <20^{o}) ionosphere (i.e., altitude range spanning ~100 km to ~800 km) hosts a number of complex and interesting phenomena; a number of which remain poorly understood. These various structures have been studied intensely since the implementation of incoherent and coherent scattering radar technologies implemented in the 1960's & by passive airglow instruments observing thermospheric emissions [e.g., Kelley, 1989]. Examples include the Equatorial Ionization Anomaly (EIA, also known as the Appleton Anomaly), the Midnight Temperature Maximum (MTM), the Pre-Reversal Enhancement (PRE), He^{+} recombination, the influence of upwardly propagating gravity waves, tidal signatures, and storm-time influx; many of which are coupled via neutral and/or electromagnetic (EM) interactions.

Furthermore, many of these phenomena are interesting for more than academic reasons. The occurrence of Equatorial Spread-F (ESF) causes scintillation in radio communications much like atmospheric turbulence causes stars to twinkle in the visible portion of the EM spectrum. This scintillation can cause a wide variety of problems, including 1) decreased satellite-to-ground message throughput and disruption of UHF and L-band communication, 2) degradation in GPS navigation performance, 3) delayed signal acquisition, and 4) radar tracking errors.

The basic physics involved with the formation and development of such scintillation has been studied for over 30 years, and there are currently a number of physical mechanisms that are suspected to cause the generation of such activity. However, the upper atmospheric community has only recently reached a level of understanding that the actual prediction and forecasting of ESF and corresponding scintillation is actually being attempted. A notable case-in-point is the Communication/Navigation Outage Forecasting System (C/NOFS) as implemented by the Air Force through the Department of Defense Space Test Program and the Air Force Research Laboratory. This program is designed to detect regions of scintillation, to forecast regions of scintillation from 3 to 6 hours in advance, and to improve our understanding of scintillation mechanisms and probability of occurrence. C/NOFS consists of three main elements: a low-inclination (13^{o}), elliptical orbit (~400 x 710 km altitude) satellite with several ionospheric instruments scheduled for launch in April 2005, a set of ground instruments for satellite calibration and validation, and forecast model development.

The C/NOFS program will, in many ways, advance our understanding of ESF, its causes, and its resultant impacts. However, we contend that there is great potential to increase the range of the forecasts beyond the limited 3 to 6 hour period. Specifically, we theorize that gravity wave seeding of instabilities in the lower thermosphere may provide the physical mechanism by which ESF is generated. If this gravity wave seeding could be predicted, then one could advance the operational range of the C/NOFS forecasting system.

Based on this theory, we are in the process of developing a unique, globally extended, synoptic gravity wave forecasting model spanning from the ground to ~400 km altitude. We call this model: the FOREcasting of Gravity waves using Ray-tracing Algorithms based on Tropospheric Sources model (i.e., the FOREGRATS model). The FOREGRATS model ingests daily analyses and 5-day forecasts from other numerical weather models in an attempt to locate, identify, & characterize tropospheric structures/sources of gravity waves. The model then prescribes an appropriate gravity wave source spectrum at the location of the sources based on current formulations in the literature. After this prescription, the individual gravity wave rays are allowed to propagate through the 3D background atmosphere using standard ray-tracing algorithms. The subsequent gravity wave activity, as indicated by modeled wind & temperature perturbations, are compiled so as to deduce regional middle and upper atmospheric gravity wave activity. We believe that the study of this gravity wave activity will lend insight to the generation of ESF.

We further explore the science of forecasting ESF in Section 3. In Section 4 we present the fundamental technical aspects of the FOREGRATS model. We summarize the current operational state of the model and present conclusions in Section 5.

3. JUSTIFICATION OF TECHNIQUE

The recent review by Fejer et al. [1999] summarizes the physics of the relationship of the F-region dynamo to the development of plasma irregularities via the Rayleigh-Taylor instability (RTI). In short, the flow of air across the evening twilight terminator, when combined with the variation of the collision frequency with height and the lack of conductivity within the intermediate E-region, will generate a zonal polarization electric field. The subsequent **E**x**B** abrupt rise [that is characteristic of the PRE] will increase the growth rate of the generalized RTI, which depends on the vertical ion drift speed, the strength of the downward vertical wind, and the magnitude of the electron gradient induced by a "seeding" perturbation [Kelley et al., 1989; Stephan et al., 2002]. As the instability develops, the F-region plasma will support the rapid growth of electron density perturbations that result in the disruption of the medium with depletions, "bubbles", and extensive scintillation and bottomside spread-F activity. Because plasma irregularities have been observed to grow more quickly than the linear RTI theory would predict, gravity waves have often been invoked as the source of the "seeding" to explain the explosive character of ESF development [e.g., Kelley et al., 1981; Hysell et al., 1990; Aggson et al., 1992; Hanson et al., 1997; Balthazor&Moffett, 1997].

3.1. ESF Generation Via Thermospheric Zonal Wind Variability Given this information, a number of current studies are looking at the timing of the mid-afternoon zonal wind reversal and the onset of ESF disturbances during the evening hours. That is, the direct determination of this reversal time would be indicative of the prospective strength of the development of the F-region dynamo. The theory is based upon the idea that an early zonal wind reversal leads to strong eastward evening zonal winds and the subsequent development of the F-region dynamo. The resulting **E**x**B** vertical ion drift increase during the evening twilight leads to the abrupt rise of the ionosphere, i.e., the PRE. Subsequently, the plasma reaches a height where the gravitational drift term is dominant in the growth rate of the RTI, and the production of ESF in the form of bubbles and bottomside spread-F would be favored. If the opposite is true, i.e., weak evening zonal winds, then the F-region dynamo, the vertical ion drift velocity, and the PRE are all relatively weak. Hence, the ESF phenomena would not be expected because the F-region plasma did not rise to a height above 300 km, for which there is a high probability of significant RTI growth & ESF development [Fejer et al., 1999; Whalen, 2002].

What then drives the zonal wind variability? There are at least two sources of variability: Tidal wave and gravity wave modulation of the zonal winds. It is well known that upper atmospheric tidal wave wind amplitudes vary greatly on daily timescales. This variability can be attributed to variation of lower and middle atmospheric sourcing mechanisms as well as wave-wave interactions in the middle and upper atmosphere, especially with global scale planetary waves and regionalized synoptic gravity wave activity. Similarly, gravity waves deposit momentum in the middle and upper atmosphere so that the zonal wind fields are subsequently modulated. The momentum deposition also depends on strength/presence of lower atmospheric gravity wave sources and the subsequent modulation of the intervening middle and upper atmospheric wind fields as modulated by tides and planetary waves. In fact, the nonlinear interactions of gravity waves and tides could greatly alter the local/regional thermospheric zonal wind pattern.

3.2. ESF Generation Through Gravity Wave Seeding: Direct Influence The occurrence of ESF may instead be more closely dependent on the direct seeding of instabilities caused by gravity waves. There have been a large number of gravity wave signatures observed in the thermosphere. For example, mid-latitude studies at the MU radar carried out by Oliver et al. [1994] have indicated convincingly that numerous gravity waves with periods of 30 to 90 minutes, vertical wavelengths of 50 to 200 km, and amplitudes of 10 to 50 m/s do appear frequently in the mid-latitude thermosphere.

If the wind perturbations from gravity waves are indeed the source of the instabilities giving rise to ESF, then their generation and propagation from the lower and middle atmosphere into the thermosphere is critically important in the forecasting of ESF. But, as stated above, such gravity waves will be strongly influenced by the sourcing mechanisms, on the background winds, and the intervening tidal and planetary wave wind fields. Such influence causes daily variability making extended forecasting of ESF difficult.

3.3. ESF Generation through Gravity Wave Seeding: Indirect Influence through Field Mapping Recently, Prakash [1999] published an interesting theory based upon the idea of the mapping of E-region electric field perturbations generated by mesosphere gravity waves into the bottomside F-region. These perturbations are thought to be generated by the interaction of mesospheric gravity wave winds with a thin E layer and a sporadic layer in the E-region. The numerical simulation carried out in this work suggests that the ΔE perturbations generated in the mesosphere and mapped to the bottomside F region have the correct spatial characteristics that are required to support the growth of seed irregularities that participate in the RTI mechanism.

3.4 Justification of FOREGRATS Given the number of possible ESF generation mechanisms listed above, one naturally asks: What then is the dominant cause of ESF? Is it synoptic, tropospheric gravity wave activity? Is it synoptic, upper atmospheric tidal wave modulation of the zonal winds? Is it middle atmospheric tidal wave modulation of the background winds, which then modulates gravity wave propagation and seeding potential? Is it tropospheric planetary wave activity that modulates gravity wave propagation characteristics and seeding potential? Is it all of the above?

As one can see, it is no wonder that the study of ESF continues 40+ years after the implementation of the incoherent scatter radar. The complex interplay across all altitude regimes makes the forecasting of ESF a difficult, but important, challenge in upper atmospheric research. We feel that the FOREGRATS model will greatly assist in our understanding of ESF by allowing the community to investigate the impacts of regional gravity wave activity in the upper atmosphere as compared to the location of ESF generation. This model will also allow for an indirect assessment of planetary wave and tidal wave contributions to the ESF generation mechanisms through the background filtering of gravity wave components.

4. APPLICATION OF THE FOREGRATS

The FOREGRATS model was built by assimilating a number of different components, as shown in Figure 1. In each subsection below we discuss these various components. We then discuss standard model operation and summarize our progress in the last sections, respectively.

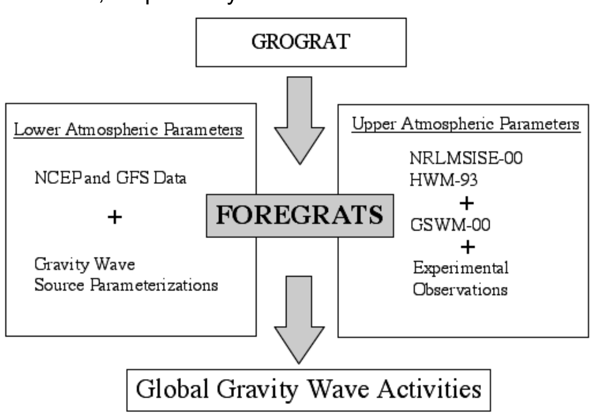

Figure 1. *Cartoon of the FOREGRATS model components and integration.*

4.1. Gravity Wave Ray-Tracing Backbone The most current FOREGRATS model (v1.3) uses the Gravity wave Regional Or Global RAy Tracer (GROGRAT) ray-tracing model, developed at the Naval Research Laboratory, as a computational backbone. The current GROGRAT ray-tracing model (v2.9) tracks the propagation and amplitude evolution of gravity waves through the lower and middle atmosphere. The original model is based on the Marks and Eckermann [1995] paper, which presented a fully non-hydrostatic gravity wave ray-tracing algorithm that included wave amplitude growth and saturation schemes. An updated version of the model formed the v2.8.1.9 GROGRAT release, which included a number of updated features [Eckermann and Marks, 1997]. Typical runs of the GROGRAT model (e.g., as in Gerrard et al. [2004a] and Brown et al. [2004]) use a traditional ray-tracing mode that made use of three-dimensional ray propagation and a one-dimensional amplitude calculation which included scale-dependent radiative damping and turbulent diffusion parameterizations and an amplitude saturation scheme. Details of the GROGRAT model can be found in the papers mentioned above.

However, as currently formulated in version v2.9, the GROGRAT model has two major issues that are currently being addressed. First, GROGRAT has a top lid of ~120 km. In order to trace gravity waves into the thermosphere, one of the initial endeavors will be to raise the upper lid to ~400 km. This will be accomplished by including the impacts of higher altitude radiative dampening, diffusion, and viscosity into the lower and middle atmospheric parameterizations of the GROGRAT model. The inclusion of ion-neutral coupling, which require an extensive adaptation of the neutral equations of motion, will also be incorporated at a later time. Currently, FOREGRATS operates under the constraint of the GROGRAT lid, though testing of the new parameterizations should be done in early 2005.

The second issue was the global nature of the proposed gravity wave forecasts. That is, the FOREGRATS model needed to be global so as to account for the impacts of gravity wave activity located from distant tropospheric sources. Though GROGRAT could run on a global grid in its native environment, the background atmospheres are interpolated with 8x8 (latitude x longitude) order spherical harmonics. This spherical harmonic fitting removed large gradient structure in the lower atmosphere and ends up smoothing “tight” atmospheric features. Though this was not a big issue in the upper atmosphere, the lower and middle atmosphere require increased accuracy to account for tropospheric fronts, convective cells, the stratospheric polar vortex, etc. To address this issue, we currently run FOREGRATS on 4 piecewise regional grids that are moved so as to cover the entire globe. This approach allows for faster regional forecasts and the use of high-spatial resolution atmospheric backgrounds. However, we must run the entire global domain at least twice so as to account for those gravity waves which leave one regional domain and enter an adjacent domain.

4.2. Background Atmosphere The background atmosphere used in FOREGRATS is obtained from a number of sources. Below ~65 km, data are obtained from the National Centers for Environmental Prediction Global Forecasting System (NCEP GFS, formally the AVN model) which are produced every 24 hours up to ~60 km altitude, and every 6 hours up to ~25 km. Above ~65 km, the atmosphere is prescribed with empirical data from the updated NRLMSISE-00 [Picone et al., 2002] and Horizontal Wind Model (HWM93 [Hedin et al., 1996]) climatologies. Time-dependent tidal amplitudes are included from Global-Scale Wave Model 2002 (GSWM-02) values [Hagan and Forbes, 2003]. When assimilated, these background fields contain the combined effects of planetary wave winds in the troposphere and middle atmosphere and tidal winds in the middle and upper atmosphere, which vary on daily and seasonal timescales.

Ideally, synoptic data obtained from instrumentation measuring winds and temperatures in the mesosphere-lower thermosphere would be assimilated into FOREGRATS. Such data assimilation schemes are in development, and should be implemented in early Spring 2005, in time to ingest data from ground-based instrumentation supporting the C/NOFS effort.

4.3. Identification of Tropospheric Gravity Wave Sources and Source Parameterization Standard atmospheric parameters like relative humidity, vertical wind velocity, geopotential height difference, and convective available potential energy (CAPE) are included as part of the standard NCEP lower atmospheric analyses. In addition, satellite products from the GOES- and AVHRR-series of spacecraft yield information on rain fall rates, locations of convection, etc. Through use of these various field diagnostics, the FOREGRATS model utilizes a 3D search algorithm to identify strong convective cells and fronts within the troposphere. Though a full description of this algorithm is beyond the scope of this paper, a coarse example of the use of these data is depicted in Figure 2(top), where we see CAPE [J/kg] analyses calculated between a layer extending from the ground to 180 hPa level at 00 UT on Oct 31, 2004 (hereafter, this example run will be referred to as the 'Halloween Run'). The locations of higher CAPE values indicate potential regions of strong convective activity, which here lies generally along the ITCZ.

These convective cells can generate a large fraction of the gravity wave activity that can propagate into the upper atmosphere [Fritts and Alexander, 2003]. That is, the gravity waves generated from such convective [and frontal] sources typically have short intrinsic periods (<45 min) and long vertical wavelengths (>20 km). Such waves tend to propagate upwards relatively quickly, so that the intervening background atmosphere tends to have less of an impact on the propagation characteristics of the gravity wave. In contrast, waves with longer intrinsic periods/shorter vertical wavelengths, generated from geostrophic adjustment or inertial-adjustment processes, propagate much more slowly, and are therefore more subject to refraction in the background wind. Furthermore, these slower propagating gravity waves are then subject to the affects of viscous and radiative dissipation much more readily than the faster portion of the gravity wave spectrum. Such dissipation would likely damp these waves before they reached sufficient altitude so as to generate the theorized seeding necessary for the generation of ESF. This is not to say that this slower part of the spectrum isn't a potentially important

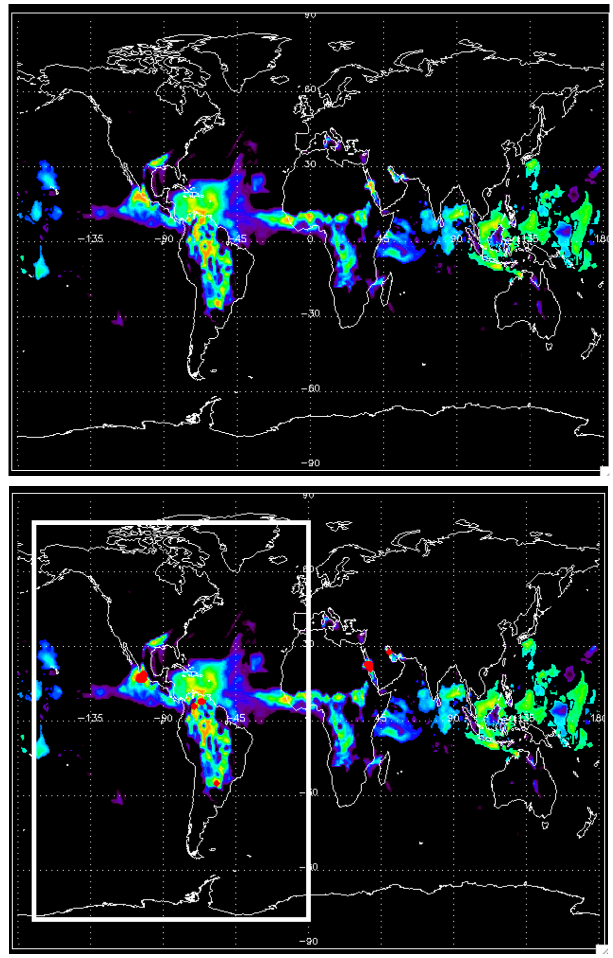

Figure 2. *(top) Global map of CAPE. Scale ranges linearly from black (= 0 J/kg) to blue to green to yellow to red (= 3500+ J/kg). (bottom) Similar to the top map, but showing the American-sector FOREGRAT model domain (white boundary) and the locations of the identified convective sources (red dots).*

component in the upper atmosphere, but rather that its influence in the upper atmosphere is likely to be less. The testing of this hypothesis alone will be an important contribution to our understanding of the influence of gravity waves in the middle and upper atmosphere.

Continuing the Halloween Run, a data processing mask, dependent on strength and structure of the CAPE, is used to identify the regions of convection. In this example, the regions of relatively strong CAPE (>2000 J/kg) are denoted with red dots in Fig. 2(bottom). These sources, now identified, are assigned an appropriate gravity wave source spectrum. This assignment is the most difficult aspect of the FOREGRATS model, as much is still not known on the nature of gravity wave source spectra. For this Halloween Run, we prescribed an ad hoc isotropic gravity wave source spectrum having horizontal wavelengths of 8.5, 12, 135.8, and 192 km and intrinsic periods of 16, 64, 128 minutes. All amplitudes were arbitrarily originally set at 0.5 m/s, and then scaled linearly depending on the magnitude of the CAPE.

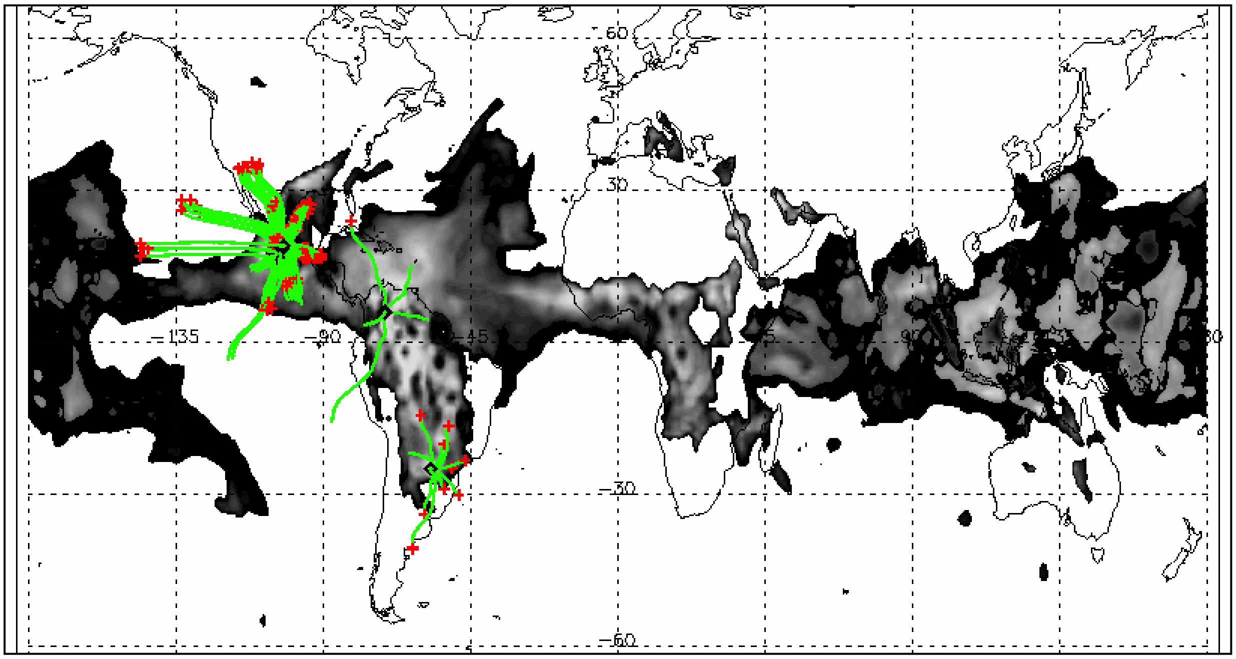

Figure 3. *Gravity wave ray-tracing results from the example Halloween run for the American sector. Green lines are ray traces, and gravity waves that reached 100 km have a red '+' at the end. These individual gravity waves were initiated with the same source spectrum, scaled in amplitude to the CAPE value from Figure 2 (bottom).*

This ad hoc source convective spectrum will be replaced with a more rigorously obtained source spectra found in the literature in the near future. For example, one convective gravity wave source spectrum can be found in the squall line simulations of Alexander et al. [1995] and Alexander [1996]. This particular source spectrum will be assigned whenever a geophysical structure analogous to a 2D squall is detected. Other such source spectra will be used for other tropospheric sources as necessary, as have been reviewed in Fritts & Alexander [2003]. For example, similar to the ad hoc spectrum used in the Halloween Run above, a "point-source" tropospheric gravity wave source spectrum will be used for isolated convective cells, whose depth of convection will determine the characteristic vertical wavelength. Multiple "point-source" tropospheric source spectra will be used to cover spatially extended systems, which is often found in the ITCZ at equatorial latitudes. This "piecewise-defined tropospheric source spectra" aspect of the FOREGRATS model will allow for future updates as more is learned about the nature of gravity wave sources.

5. CURRENT STATE OF FOREGRATS OPERATIONS

Once operational, the FOREGRATS model will be run in a 5-day forecast mode, using both NCEP GFS analyses and forecasts to make real-time gravity wave forecasts. These forecasts will be posted to the Penn State Dept. of Meteorology e-WALL, a real-time, online weather server. Enhancement of model configuration and gravity wave source prescriptions are expected to continue through the first years of operation.

The primary model data products will be 3D [global] maps of gravity wave activities, as defined by both momentum deposition and by gravity wave wind variability. For example, finishing our Halloween Run, Figure 3 depicts the results of the gravity wave ray traces through the lower and middle atmosphere, up to 100 km. Gravity waves that penetrated the 100 km altitude are denoted with a red '+', while waves that did not reach this altitude stop. At each point along each gravity wave ray path, the GROGRAT model backbone kept track of horizontal wind amplitude and momentum flux, allowing contour maps of these products to be produced. These maps will be regularly updated as the background atmosphere is updated and the FOREGRATS model is recycled.

The FOREGRATS model is about mid-way through completion. As demonstrated in the Halloween Run, the base infrastructure of the model has been finalized and is running smoothly with user guidance. Currently, global gravity wave forecasts within the middle atmosphere are being made on trial runs.

Tasks yet to be completed before FOREGRATS goes into an operational mode include:

1) The testing of higher altitude parameterizations associated with raising the top lid of the GROGRAT model,
2) Finalizing of the prescription of various tropospheric source spectra and integrate these modules into FOREGRATS,
3) Automation of model initialization and run

Given these task, we realistically expect model operation by June 2005.

6. CONCLUSIONS

For completeness, we note that the results from the FOREGRATS model need not only be applied to the study of ESF generation, but can also be applied to other scientific studies as needed. Since the global model identifies all possible convective and frontal gravity wave sources, the impacts of these waves on, for example, high latitude mesospheric clouds [Gerrard et al., 2004a,b], the generation of mesospheric inversion layers [Meriwether and Gerrard, 2004], or mesospheric fronts [Brown et al., 2004] can also be studied. This large number of spin-off science applications further warrants the development of the FOREGRATS modeling endeavor.

As applied herein to the prediction of ESF, the FOREGRATS model will increase our understanding of ESF generation, gravity wave generation and propagation, and data assimilation of mesospheric–lower thermospheric synoptic variables. This is a true statement regardless of actual forecast success or failure, as either outcome provides insight into the various processes under study. However, given the thought and care that has been put into the FOREGRATS model, we expect that this particular modeling approach will yield vital insight into the possibility of extending ESF forecasts beyond the currently sought after 4-6 hour period.

7. REFERENCES

Alexander, M. J., J. R. Holton, and D. R. Durran, The gravity wave response above deep convection in a squall line simulation, J. Atmos. Sci., 52, 2212, 1995.

Alexander, M. J., A simulated spectrum of convectively generated gravity waves: Propagation from the troposphere to the mesopause and effects on the middle atmosphere, J. Geophys. Res., 1571, 1996.

Balthazor, R.L., and R. J. Moffett, A study of atmospheric gravity waves and travelling ionospheric disturbances at equatorial latitudes, Ann. Geophys., 15, 1048-1056, 1997

Brown, L. B., A. J. Gerrard, J. W. Meriwether, and J. J. Makela, All-sky imaging observations of mesospheric fronts in OI 557.7 nm and broadband OH airglow emissions: Analysis of frontal structure, atmospheric background conditions, and potential sourcing mechanisms, J. Geophys. Res., 109, D19104, doi:10.1029/2003JD004223, 2004.

Eckermann, S. D. and C. J. Marks, GROGRAT: A new model of the global propagation and dissipation of atmospheric gravity waves, Adv. Space Res., 20, 1253-1256, 1997.

Fejer, B. J., L. Scherliess, and E. R. de Paula, Effects of the vertical plasma drift velocity on the generation and evolution of equatorial spread F, J. Geophys. Res., 104, 19,859-19,869, 1999.

Fritts, D. C., M. J. Alexander, Gravity wave dynamics and effects in the middle atmosphere, Rev. Geophys. 41, 1, 10.1029/2001RG000106, 2003.

Gerrard, A. J., T. J. Kane, S. D. Eckermann, and J. P. Thayer, Gravity waves and mesospheric clouds in the summer middle atmosphere: A comparison of lidar measurements and ray modeling of gravity waves over Sondrestrom, Greenland, J. Geophys. Res., D1010310.1029/2002JD002783, 2004a.

Gerrard, A. J., T. J. Kane, J. P. Thayer, and S. D. Eckermann, Concerning the upper stratospheric gravity wave and mesospheric cloud relationship over Sondrestrom, Greenland, J. Atmos. Solar-Terr.Phys., 66, 229-240, 2004b.

Hagan, M. E. and J. M. Forbes, Migrating and nonmigrating semidiurnal tides in the upper atmosphere excited by tropospheric latent heat release, J. Geophys. Res., 108(A2), 1062, doi:10.1029/2002JA009466, 2003.

Hanson, W. B., W. R. Coley, R. A. Heelis, and A. Urquhart, Fast equatorial bubbles, J. Geophys. Res., 102, 2039, 1997.

Hedin, A. E., E.L. Fleming, A.H. Manson, F.J. Scmidlin, S.K. Avery, R.R. Clark, S.J. Franke, G.J. Fraser, T. Tsunda, F. Vial and R.A. Vincent, Emperical Wind Model for the Upper, Middle, and Lower Atmosphere, J. Atmos. Terr. Phys., 58, 1421-1447, 1996.

Hysell, D., M. C. Kelley, W. E. Swartz, and R. F. Woodman, Seeding and layering of equatorial spread F by gravity waves, J. Geophys. Res., 17,253, 1990.

Kelley, M. C., M. F. Larsen, C. A. Lahoz, J. P. McClure, gravity wave initiation of equatorial spread F, J. Geophys. Res., 84, 9087, 1981.

Kelley, M. C., The Earth's Ionosphere, Academic Press, 1989.

Marks, C. J., and S. D. Eckermann, A three dimensional nonhydrostatic ray-tracing model for gravity waves: Formulation and preliminary results for the middle atmosphere, J. Atmos. Sci., 52, 1959-1984, 1995.

Meriwether, J. W., and A. J. Gerrard, Mesosphere inversion layers and stratosphere temperature enhancements, Rev. Geophys., 42, RG3003, doi:10.1029/2003RG000133, 2004.

Oliver, W. L., S. Fukao, Y. Yamamoto, T. Takami, M.D. Yamanaka, M. Yamamoto, T. Nakamura, and T. Tsuda, Middle and upper atmosphere radar observations of ionospheric density gradients produced by gravity wave packets, J. Geophys. Res., 99, 6321-6329, 1994.

Picone, J. M., A.E. Hedin, D.P. Drob, and A.C. Aikin, NRLMSISE-00 empirical model of the atmosphere: Statistical comparisons and scientific issues, J. Geophys. Res., 107(A12), 1468, doi:10.1029/2002JA009430, 2002.

Prakash S., Production of electric field perturbations by gravity wave winds in the E region suitable for initiating equatorial spread-F, J. Geophys. Res., 104, 10,051-10,069, 1999.

Stephan, A. W., M. Colerico, M. Mendillo, B. W. Reinisch, and D. Anderson, Suppression of equatorial spread F by sporadic E, J. Geophys. Res., 107, 2002

Waldock, J. A., Wind and temperature effects on F-region medium-scale gravity waves estimated using a multi-layer atmospheric model, J. Atmos. Sol. Terr. Phys., 58, 11, 1259-1273,1996.

Whalen, J. A., Dependence of equatorial bubbles and bottomside spread F on season, magnetic activity, and ExB drift velocity during solar maximum, Geophys. Res. Lett., 21, ,2002.